

ANALYTICAL AND NUMERICAL DETERMINATION OF THE FULL DYNAMIC REACTIONS IN THE BEARING SUPPORTS OF BIG BAND SAW MACHINES

BOYCHO MARINOV*

*Institute of Mechanics, Bulgarian Academy of Sciences,
Acad. G. Bonchev St., Bl. 4, 1113 Sofia, Bulgaria*

[16 February 2021. Accepted: 20 September 2021

ABSTRACT: In this paper, the influence of dynamic loads that cause dynamic reactions in the upper shaft supports of big band saw machines is investigated. These loads are created by the dynamic forces and moments that occur in operating mode, as well as by the kinematic and mass characteristics of the rotating disk. Expressions for calculation of the dynamic reactions caused by the external load are obtained, as well as expressions for calculation of the dynamic reactions due to the change of the kinematic and mass characteristics of the leading wheel. With the help of these expressions, final expressions to calculate the full dynamic reactions in the bearing supports are obtained. Using the obtained analytical expressions, planar and spatial diagrams are constructed, which show the change of the full dynamic reactions when changing different parameters.

KEY WORDS: band saw machines, external load, normal and cutting forces, kinematics and mass characteristics, dynamic reactions.

1 INTRODUCTION

The band saw machines are a certain class of woodworking machines for longitudinal, cross or curvilinear sawing. They are used for sawing logs, boards, slabs, prisms, details etc. These machines saw the workpiece through a band saw blade and two leading wheels. According to the diameters of the two wheels and the width of the band saw blade, band saw machines are divided into three groups: ordinary band saw machines, deal band saw machines and log band saw machines or big band saw machines.

In this work, the full dynamic reactions in the bearing supports of big band saw machines are analyzed. These reactions are caused by both the external load and the kinematic and mass characteristics of the rotating disk. Research related to the determination of the external loads that form the dynamic reactions in main links of some classes of woodworking machines are published in the technical literature [1–6].

*Corresponding author e-mail: boicho_marinoff@yahoo.co.uk

The purpose of this study is to obtain expressions for calculating the full dynamic reactions in the bearing supports of the upper leading wheel. In order to achieve this purpose, the following main tasks must be fulfilled:

- obtaining expressions for calculating the dynamic reactions due to the external load;
- obtaining expressions for calculating the dynamic reactions due to the kinematic and mass characteristics of the rotating disk;
- obtaining expressions for calculating the full dynamic reactions in the bearing supports of the upper shaft and drawing planar and spatial diagrams that show the dependence of these reactions on different parameters.

2 EXPOSE

To solve the problems posed, a scheme of the cutting mechanism of the band saw machine is presented. The dynamic models are also presented. These models are used to determine the dynamic reactions caused by external loads and the kinematic and mass characteristics of the rotating disk.

2.1 SCHEME OF THE CUTTING MECHANISM

The scheme of the cutting mechanism is shown in Fig. 1 [7, 8].

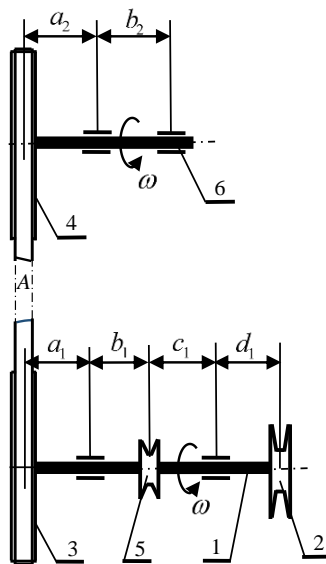


Fig. 1: Cutting mechanism.

The following symbols are defined: 1 – main shaft; 2 and 5 – belt pulleys; 3 and 4 – leading wheels; A – band saw blade, and 6 – upper shaft.

2.2 DYNAMIC MODEL

Figure 2 shows the dynamic model when the upper leading wheel is mounted at the end of the upper shaft.

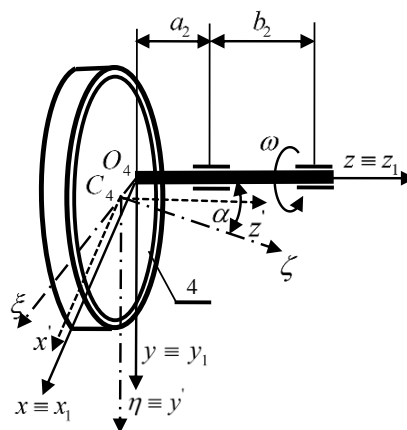


Fig. 2: Dynamic model.

The following coordinate systems are used to obtain expressions for calculating the full dynamic reactions [9]:

- fixed coordinate system O_4xyz and moving coordinate system $O_4x_1y_1z_1$. In the initial moment the axes of the two coordinate systems coincide;
- coordinate system $C_4x'y'z'$, whose axes are parallel to the axes of the moving coordinate system;
- coordinate system $C_4\xi\eta\zeta$. The axes of this coordinate system are principal axes of inertia.

The linear and angular deviations e and α are also shown in the figure as $e = O_4C_4$ and α is the angle between the axes ζ and z .

2.3 DYNAMIC REACTIONS CAUSED BY EXTERNAL LOAD

We consider the external forces that load the leading wheel 4. These forces are shown in Fig. 3.

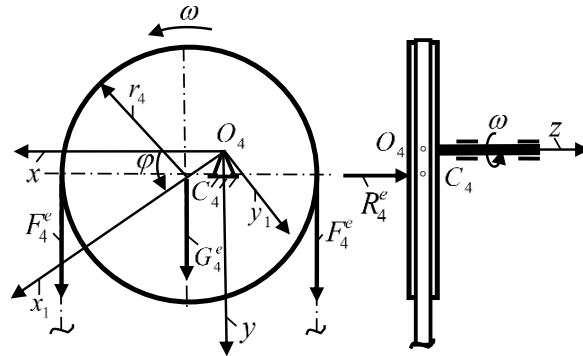


Fig. 3: External load on the leading wheel.

The leading wheel rotates with a constant angular velocity ω and describes an angle $\phi = \omega t$. The tensile forces in the band saw blade are denoted by F_4^e . Difference expressions for calculating this force are presented in the technical literature. An appropriate formula for its calculation is written below [7].

$$(1) \quad F_4^e = 1.5N_c/V ,$$

where N_c is the cutting power and V is the cutting speed.

The weight of the leading wheel is denoted by G_4^e and can be calculated from a formula known in literature [10, 11].

$$(2) \quad G_4^e = m_4g ,$$

where m_4 is the mass of the leading wheel 4 and g is the acceleration of gravity.

The force R_4^e is transmitted from band saw blade to the leading wheel. This force can be calculated with sufficient accuracy from the next dependence [7]

$$(3) \quad R_4^e = \frac{R_b^n + R_\Sigma}{2} ,$$

where R_Σ is the total resistance force. This force is calculated for each individual case. R_b^n is the normal force loading the workpiece. This force can be calculated from the expression below, in which the cutting force P_b^τ participates [7, 12]

$$(4) \quad R_b^n = mP_b^\tau = m \frac{K_{\Delta(\lambda)}bHu}{V} ,$$

where H is the thickness of the workpiece, u is the feeding speed, b is the width of the cutter, m is a coefficient that changes within the following limits $0 \leq m \leq 1$. $K_{\Delta(\lambda)}$

is the specific work of the cutting. It is determined from the next expressions [13]

$$(5) \quad K_{\Delta} = k + \frac{a_{\rho} p}{u_{z\Delta}} + \frac{\alpha_{\Delta} H}{b}, \quad K_{\lambda} = k + \frac{a_{\rho} p s}{b u_{z\lambda}} + \frac{\alpha_{\lambda} H}{b}.$$

The symbol $\alpha_{\Delta(\lambda)}$ is the friction intensity of the shavings on the sawing walls, as α_{Δ} is used for swage-set teeth and α_{λ} – for part-set teeth. a_{ρ} is a coefficient of the blunt teeth, s is a thickness of the band saw blades. k is the fictitious pressure on the front side of the teeth and p is the fictitious specific force on the back side of the teeth. The feeding of one tooth is marked with $u_{z\Delta}$, $u_{z\lambda}$.

To determine the dynamic reactions, we first determine the load on the upper shaft of the band saw machine. For this purpose, we reduce the forces that load the leading wheel to the axis of rotation of the upper shaft. Figure 4 shows the forces and moments that load the shaft and cause the dynamic reactions in the bearing supports. These reactions are also shown.

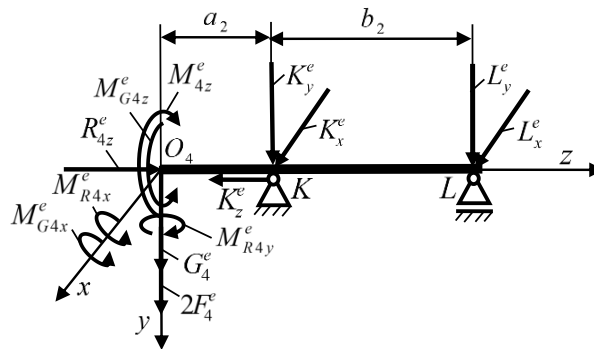


Fig. 4: Loading the upper shaft.

The force R_{4z}^e is calculated from the following expression:

$$(6) \quad R_{4z}^e = R_4^e \cos \alpha.$$

This force creates the following moments relative to the axes x , y and z .

$$(7) \quad \begin{aligned} M_{R4x}^e &= \frac{1}{2} \left(\frac{m K_{\Delta(\lambda)} b H u}{V} + R_{\Sigma} \right) e \cos \alpha \sin \omega t, \\ M_{R4y}^e &= \frac{1}{2} \left(\frac{m K_{\Delta(\lambda)} b H u}{V} + R_{\Sigma} \right) \cos \alpha (r_4 + e \cos \omega t), \\ M_{R4z}^e &= 0. \end{aligned}$$

The weight of the leading wheel G_4^e creates moments relative to the axes x , y and z presented below:

$$(8) \quad \begin{aligned} M_{G_4x}^e &= m_4ge \sin \alpha, \\ M_{G_4y}^e &= 0, \\ M_{G_4z}^e &= m_4ge \cos \alpha \cos \omega t. \end{aligned}$$

Dynamic reactions can be determined from the equilibrium conditions. From these conditions, we obtain the corresponding equations in which the support reactions participate.

$$(9) \quad \begin{aligned} R_{4z}^e - K_z^e &= 0, \\ M_{G_4x}^e + M_{R_4x}^e + G_4^e a_2 + 2F_4^e a_2 - L_y^e b_2 &= 0, \\ M_{G_4x}^e + M_{R_4x}^e + G_4^e (a_2 + b_2) + 2F_4^e (a_2 + b_2) + K_y^e b_2 &= 0, \\ -M_{R_4y}^e + L_x^e b_2 &= 0, \\ -M_{R_4y}^e - K_x^e b_2 &= 0. \end{aligned}$$

After performing some substitutions, we get the expressions for the dynamic reactions caused by the external load in a final form. These expressions are presented below:

$$(10) \quad \begin{aligned} K_z^e &= \left(\frac{mK_{\Delta(\lambda)}bHu}{V} + R_\Sigma \right) \frac{\cos \alpha}{2}, \\ L_y^e &= \frac{m_4g}{b_2} (a_2 + e \sin \alpha) + \frac{3N_c a_2}{b_2 V} \\ &\quad + \frac{1}{2b_2} \left(\frac{mK_{\Delta(\lambda)}bHu}{V} + R_\Sigma \right) e \cos \alpha \sin \omega t, \\ K_y^e &= -\frac{m_4g}{b_2} (a_2 + b_2 + e \sin \alpha) - \frac{3N_c (a_2 + b_2)}{b_2 V} \\ &\quad - \frac{1}{2b_2} \left(\frac{mK_{\Delta(\lambda)}bHu}{V} + R_\Sigma \right) e \cos \alpha \sin \omega t, \\ L_x^e &= \frac{r_4}{2b_2} \left(\frac{mK_{\Delta(\lambda)}bHu}{V} + R_\Sigma \right) \cos \alpha \\ &\quad + \frac{1}{2b_2} \left(\frac{mK_{\Delta(\lambda)}bHu}{V} + R_\Sigma \right) e \cos \alpha \cos \omega t, \\ K_x^e &= -\frac{r_4}{2b_2} \left(\frac{mK_{\Delta(\lambda)}bHu}{V} + R_\Sigma \right) \cos \alpha \\ &\quad - \frac{1}{2b_2} \left(\frac{mK_{\Delta(\lambda)}bHu}{V} + R_\Sigma \right) e \cos \alpha \cos \omega t. \end{aligned}$$

2.4 DYNAMIC REACTIONS CAUSED BY THE KINEMATIC AND MASS CHARACTERISTICS OF THE ROTATING DISK

To determine the dynamic reactions caused by the kinematic and mass characteristics of the leading wheel, we use the dynamic model, shown in Fig. 5.

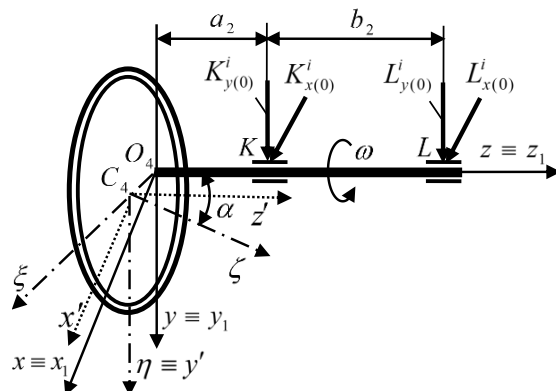


Fig. 5: Dynamic model.

Dynamic reactions can be determined by the following equations [10]:

$$\begin{aligned}
 m_4 \left(-\varepsilon y_{C_4}^{(0)} - \omega^2 x_{C_4}^{(0)} \right) &= K_{x(0)}^i + L_{x(0)}^i, \\
 m_4 \left(\varepsilon x_{C_4}^{(0)} - \omega^2 y_{C_4}^{(0)} \right) &= K_{y(0)}^i + L_{y(0)}^i, \\
 -\varepsilon J_{xz}^{(0)} + \omega^2 J_{yz}^{(0)} &= -K_{y(0)}^i a_2 - L_{y(0)}^i (a_2 + b_2), \\
 -\varepsilon J_{yz}^{(0)} - \omega^2 J_{xz}^{(0)} &= K_{x(0)}^i a_2 + L_{x(0)}^i (a_2 + b_2).
 \end{aligned}
 \tag{11}$$

The following symbols are used: $x_{C_4}^{(0)}$ and $y_{C_4}^{(0)}$ are the coordinates of the center of mass C_4 in the initial moment. The centrifugal moments of the leading wheel about axes x, z and y, z in the initial moment are denoted by $J_{xz}^{(0)}$ and $J_{yz}^{(0)}$.

We consider motion with constant angular velocity, i.e., $\omega = \text{const}$, $\varepsilon = 0$, where ε is the angular acceleration. In this case, the dynamic reactions are constant with respect to the moving coordinate system. These reactions change about the fixed coordinate system depending on the change in the angle ϕ . We can determine their sizes to an arbitrary position. Therefore, we choose the initial position when $\phi = 0$. For this position, the axes of the fixed coordinate system O_4xyz and the moving coordinate system $O_4x_1y_1z_1$ coincide. In this case, the coordinates of the centre of mass C_4 are calculated by the following expressions:

$$x_{C_4}^{(0)} = e \cos \alpha, \quad y_{C_4}^{(0)} = 0, \quad z_{C_4}^{(0)} = -e \sin \alpha.
 \tag{12}$$

The centrifugal moments $J_{xz}^{(0)}$ and $J_{yz}^{(0)}$ for the initial position ($\phi = 0$) can be calculated using the Huygens-Steiner theorem [10, 11].

$$(13) \quad \begin{aligned} J_{xz}^{(0)} &= J_{x'z'}^{(0)} + m_4 x_{C_4}^{(0)} z_{C_4}^{(0)}, \\ J_{yz}^{(0)} &= J_{y'z'}^{(0)} + m_4 y_{C_4}^{(0)} z_{C_4}^{(0)}, \end{aligned}$$

where $J_{x'z'}^{(0)}$ and $J_{y'z'}^{(0)}$ are the centrifugal moments relative to the respective axes of the coordinate system $C_4x'y'z'$. After corresponding transformations, we get expressions about the centrifugal moments in final form

$$(14) \quad \begin{aligned} J_{xz}^{(0)} &= \frac{1}{2} (J_\xi - J_\zeta - m_4 e^2) \sin 2\alpha, \\ J_{yz}^{(0)} &= 0, \end{aligned}$$

where J_ξ and J_ζ are the mass moments of inertia of the rotating disk toward axes ξ and ζ .

After the explanations made above, we can write the expressions (11) in the following form:

$$(15) \quad \begin{aligned} -m_4 \omega^2 e \cos \alpha &= K_{x(0)}^i + L_{x(0)}^i, \\ 0 &= K_{y(0)}^i + L_{y(0)}^i, \\ 0 &= -K_{y(0)}^i a_2 - L_{y(0)}^i (a_2 + b_2), \\ -\frac{\omega^2}{2} (J_\xi - J_\zeta - m_4 e^2) \sin 2\alpha &= K_{x(0)}^i a_2 + L_{x(0)}^i (a_2 + b_2). \end{aligned}$$

From these expressions, we obtain the expressions for the dynamic reactions for the initial position ($\phi = 0$) in the final form

$$(16) \quad \begin{aligned} K_{x(0)}^i &= -\frac{\omega^2}{b_2} \left[(a_2 + b_2 + e \sin \alpha) m_4 e \cos \alpha - \frac{1}{2} (J_\xi - J_\zeta) \sin 2\alpha \right], \\ L_{x(0)}^i &= \frac{\omega^2}{b_2} \left[(a_2 + e \sin \alpha) m_4 e \cos \alpha - \frac{1}{2} (J_\xi - J_\zeta) \sin 2\alpha \right], \\ K_{y(0)}^i &= L_{y(0)}^i = 0. \end{aligned}$$

The dynamic reactions for an arbitrary position ($\phi \neq 0$) can be determined from the following dependencies:

$$(17) \quad \begin{aligned} K_x^i &= K_{x(0)}^i \cos \omega t, & K_y^i &= K_{x(0)}^i \sin \omega t, \\ L_x^i &= L_{x(0)}^i \cos \omega t, & L_y^i &= L_{x(0)}^i \sin \omega t. \end{aligned}$$

We can write the expressions for the dynamic reactions in final form using the dependencies (16) and (17).

$$\begin{aligned}
K_x^i &= -\frac{\omega^2}{b_2} \left[(a_2 + b_2 + e \sin \alpha) m_4 e \cos \alpha - \frac{1}{2} (J_\xi - J_\zeta) \sin 2\alpha \right] \cos \omega t, \\
K_y^i &= -\frac{\omega^2}{b_2} \left[(a_2 + b_2 + e \sin \alpha) m_4 e \cos \alpha - \frac{1}{2} (J_\xi - J_\zeta) \sin 2\alpha \right] \sin \omega t, \\
L_x^i &= \frac{\omega^2}{b_2} \left[(a_2 + e \sin \alpha) m_4 e \cos \alpha - \frac{1}{2} (J_\xi - J_\zeta) \sin 2\alpha \right] \cos \omega t, \\
L_y^i &= \frac{\omega^2}{b_2} \left[(a_2 + e \sin \alpha) m_4 e \cos \alpha - \frac{1}{2} (J_\xi - J_\zeta) \sin 2\alpha \right] \sin \omega t.
\end{aligned}
\tag{18}$$

2.5 FULL DYNAMIC REACTIONS

The full dynamic reactions can be calculated by using expressions (10) to calculate the dynamic reactions caused by external loads and expressions (18) to calculate the dynamic reactions caused by the kinematic and mass characteristics of the rotating disk. We write these expressions in final form after appropriate transformations

$$\begin{aligned}
K_x &= -\frac{r_4}{2b_2} \left(\frac{mK_{\Delta(\lambda)}bHu}{V} + R_\Sigma \right) \cos \alpha \\
&\quad - \left\{ \frac{1}{2b_2} \left(\frac{mK_{\Delta(\lambda)}bHu}{V} + R_\Sigma \right) e \cos \alpha \right. \\
&\quad \left. + \frac{\omega^2}{b_2} \left[(a_2 + b_2 + e \sin \alpha) m_4 e \cos \alpha - \frac{1}{2} (J_\xi - J_\zeta) \sin 2\alpha \right] \right\} \cos \omega t, \\
K_y &= -\frac{m_4 g}{b_2} (a_2 + b_2 + e \sin \alpha) - \frac{3N_c(a_2 + b_2)}{b_2 V} \\
&\quad - \left\{ \frac{1}{2b_2} \left(\frac{mK_{\Delta(\lambda)}bHu}{V} + R_\Sigma \right) e \cos \alpha \right. \\
&\quad \left. + \frac{\omega^2}{b_2} \left[(a_2 + b_2 + e \sin \alpha) m_4 e \cos \alpha - \frac{1}{2} (J_\xi - J_\zeta) \sin 2\alpha \right] \right\} \sin \omega t, \\
L_x &= \frac{r_4}{2b_2} \left(\frac{mK_{\Delta(\lambda)}bHu}{V} + R_\Sigma \right) \cos \alpha \\
&\quad + \left\{ \frac{1}{2b_2} \left(\frac{mK_{\Delta(\lambda)}bHu}{V} + R_\Sigma \right) e \cos \alpha \right. \\
&\quad \left. + \frac{\omega^2}{b_2} \left[(a_2 + e \sin \alpha) m_4 e \cos \alpha - \frac{1}{2} (J_\xi - J_\zeta) \sin 2\alpha \right] \right\} \cos \omega t, \\
L_y &= \frac{m_4 g}{b_2} (a_2 + e \sin \alpha) + \frac{3N_c a_2}{b_2 V} + \left\{ \frac{1}{2b_2} \left(\frac{mK_{\Delta(\lambda)}bHu}{V} + R_\Sigma \right) e \cos \alpha \right. \\
&\quad \left. + \frac{\omega^2}{b_2} \left[(a_2 + e \sin \alpha) m_4 e \cos \alpha - \frac{1}{2} (J_\xi - J_\zeta) \sin 2\alpha \right] \right\} \sin \omega t.
\end{aligned}
\tag{19}$$

3 NUMERICAL EXAMPLE

The results of the carried-out computer experiments are presented in Figs. 6 and 7. We use the following initial data [13–16]: $\omega = 56 \text{ s}^{-1}$, $e = \{0, 0.001\} \text{ m}$, $\alpha = \{0, 0.017\} \text{ rad}$, $a_2 = 0.4 \text{ m}$, $b_2 = 0.8 \text{ m}$, $m_4 = 810 \text{ kg}$, $J_\xi = 171 \text{ kg m}^2$, $J_\zeta = 336 \text{ kg m}^2$, $N_c = 43,4 \text{ kW}$, $V = 45 \text{ m/s}$, $r_4 = 0.8 \text{ m}$, $s = 1.47 \text{ mm}$, $b = 2.5 \text{ mm}$, $p = 9220 \text{ N/m}$, $k = 35 \times 10^6 \text{ Pa}$, $\alpha_\lambda = 245 \times 10^3 \text{ Pa}$, $\alpha_\Delta = 196 \times 10^3 \text{ Pa}$, $m = 0.5$, $H = 0.42 \text{ m}$, $u = 0.5 \text{ m/s}$, $u_{z\Delta} = 2.5 \text{ mm}$, $K_\Delta = 80 \times 10^6 \text{ J/m}^3$, $R_\Sigma = 2400 \text{ N}$.

3.1 PLANE DIAGRAMS

Figure 6 shows the plane diagrams of the full dynamic reactions K_x , K_y , L_x , L_y .

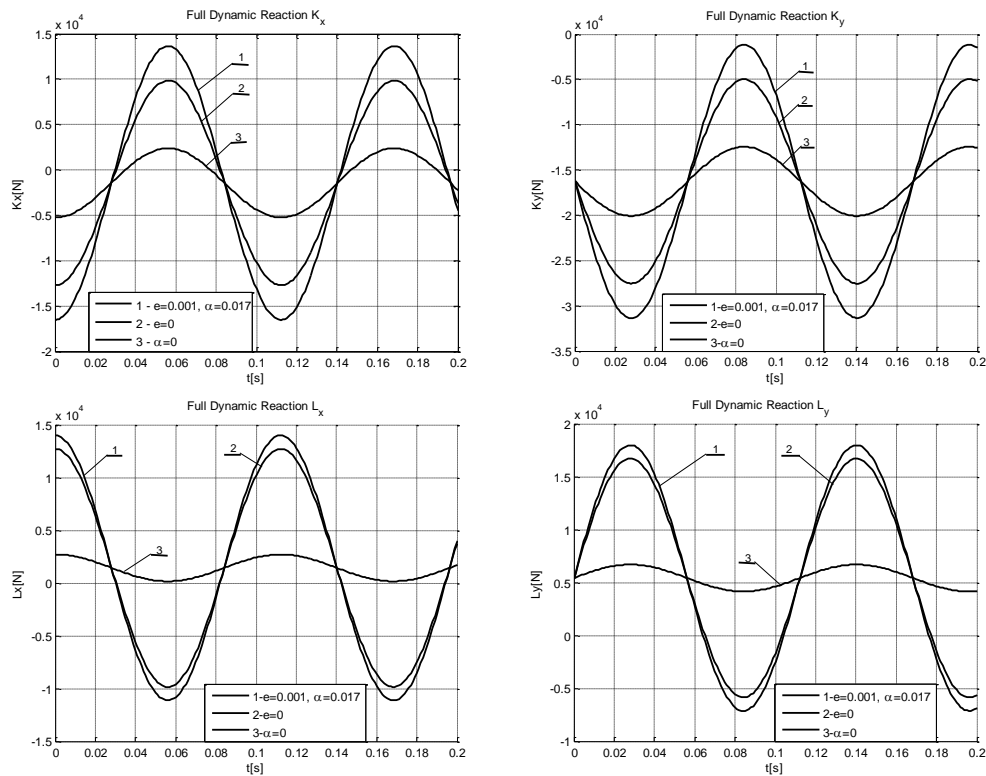


Fig. 6: Plane diagrams of the full dynamic reactions K_x , K_y , L_x , L_y .

3.2 SPATIAL DIAGRAM

Figure 7 shows the spatial diagrams of the full dynamic reactions K_x , K_y , L_x , L_y .

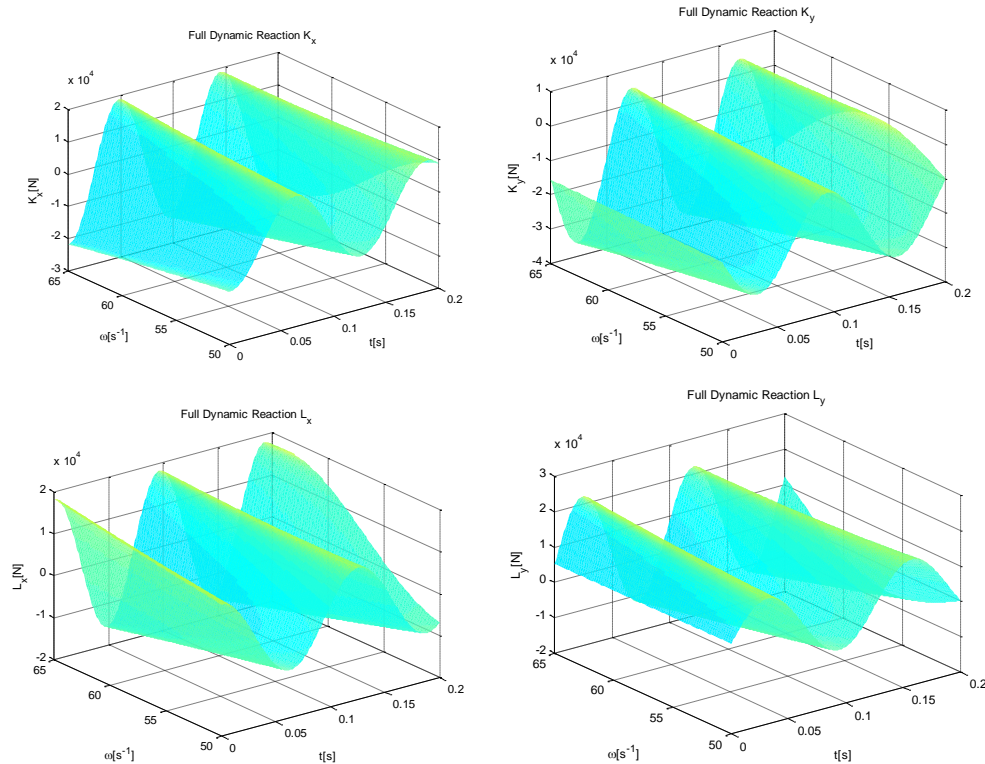


Fig. 7: Spatial diagrams of the full dynamic reactions K_x , K_y , L_x , L_y .

4 ANALYSIS OF THE OBTAINED RESULTS

In this paper, analytical expressions for calculating the full dynamic reactions are obtained. With the help of these expressions, plane and spatial diagrams are constructed, which show the change of these reactions when different parameters change. The plane diagrams presented in Fig. 6 show how the dynamic reactions change as a function of time t . These diagrams are constructed at different values of the two parameters e and α . We can establish that the angular deviations affect the magnitudes of the reactions much more than the linear deviations. This fact can be used in the design of new band saw machines. These diagrams also show that dynamic reactions take on both positive and negative values. This is a very unfavorable operating mode because it can lead to the so-called material fatigue phenomenon and, consequently, to the destruction of the machine shaft.

The spatial diagrams presented in Fig. 7 show how the dynamic reactions change when the two arguments change, i.e., when the time t and the angular velocity ω

change. These diagrams are constructed when the linear and angular deviations assume maximum values. We can find that as the angular velocity increases, the magnitudes of the dynamic reactions also increase. This is due to the fact that in this case the magnitudes of inertial forces and moments increase.

The obtained theoretical expressions can be used in different cases.

- Strength dimensioning or strength check of the upper shaft of the band saw machine [17, 18];

For this purpose, the maximum equivalent stress $\max \sigma_e$ must be calculated using the following dependence:

$$(20) \quad \max \sigma_e = \frac{\max M_e}{W_b},$$

where W_b is the section modulus. $\max M_e$ is the maximum equivalent moment. This moment is calculated using the obtained expressions for the full dynamic reactions.

The maximum equivalent stresses must be compared with the permissible stresses

$$(21) \quad \max \sigma_e \leq [\sigma].$$

This expression can be used to make strength dimensioning when designing new band saw machines or to perform a strength check for existing machines.

- Deformation check of the upper shaft of the band saw machine [17, 18];

The following inequalities are used in this case:

$$(22) \quad f_{\max} \leq [f], \quad f_{\max}/l_b \leq [f/l_b],$$

where $[f]$ is the admissible deflection and $[f/l_b]$ is the admissible relative deflection. f_{\max} is the maximum deflection. This deflection is calculated using the obtained expressions for the full dynamic reactions.

The above inequalities can be used to make a deformation check when designing new band saw machines or to perform a deformation check for existing machines.

- Study of the transverse vibrations and spatial deformations of the upper shaft;

In this case, the transverse vibrations of the shaft in two mutually perpendicular planes can be investigated using the following expressions:

$$(23) \quad x_i(z, t) = Z_{1i}(z) \cos \omega t, \quad y_i(z, t) = Z_{2i}(z) \sin \omega t, \quad (i = 1, 2).$$

The functions Z_{1i} and Z_{2i} can be determined using the analytical expressions obtained in this article. With the help of the above expressions, the spatial deformations of the upper shaft can also be determined.

- Optimal placement of the leading wheel and suitable disposal of the bearing supports and achieving the minimum dimensions of the mechanical system.

5 CONCLUSIONS

In this paper, the full dynamic reactions that occur in the bearing supports of big band saw machines are analyzed. The main purpose of the research is formulated, as well as the main tasks to be solved. A scheme of the cutting mechanism is presented for the performance of these tasks. The corresponding dynamic models are also shown. In order to fulfill the first main task formulated in the introductory part of the study, the external forces that load the upper leading wheel are analyzed. These forces, as well as the dynamic moments generated by them, are reduced by the axis of rotation. With the help of the equilibrium conditions and the corresponding equations, expressions for calculating the dynamic reactions caused by the external load are obtained.

To solve the second main task, the corresponding dynamic model is built. The equations in which the dynamic reactions caused by the kinematic and mass characteristics of the rotating disk participate are written. After corresponding transformations, expressions for calculation of the dynamic reactions in the initial position ($\phi = 0$) are obtained. From these expressions, dependencies for calculating the dynamic reactions for an arbitrary position ($\phi \neq 0$) are obtained.

With the help of the obtained dependencies, the third main task is solved. These dependencies are used to obtain expressions for calculating the full dynamic reactions in the bearing supports of the upper leading wheel in final form. The corresponding plane and spatial diagrams are drawn, which show how the respective dynamic reactions change when different parameters change.

In conclusion, we can say that the obtained theoretical expressions and the drawn diagrams can be used both in the design of new ban saw machines and in existing machines to improve their safe and reliable operation.

REFERENCES

- [1] W. ZHENG, J. BEN-HAO, Y. XIAO-JUN (2012) Dynamic tensile force survey of wood-working band saw blades. *International Conference on Solid State and Materials Lecture, Notes in Information Technology*. Nanjing, China, **22** 31-37.
- [2] R. MARCHAL, F. MOTHE, L.-E. DENAUD, B. THIBAUT, L. BLERON (2009) Cutting forces in wood machining – Basics and applications in industrial processes. A review COST Action E35 2004–2008: Wood machining – micromechanics and fracture. *Holz-forschung* **63**(2) 157-167; DOI:10.1515/HF.2009.014.
- [3] B. PORANKIEWICZ, G. GOLI (2014) Cutting forces by oak and douglas fir machining. *Maderas. Ciencia y tecnologia* **16**(2) 199-216; DOI:10.4067/S0718-221X2014005000016.
- [4] L. HLÁSKOVÁ, K. ORLOWSKI, Z. KOPECKÝ, M. JEDINÁK (2015) Sawing processes as a way of determining fracture toughness and shear yield stresses of wood. *BioResources* **10**(3) 5381-5394; DOI:10.15376/biores.10.3.5381-5394.

- [5] P. MORADPOUR, F. SCHOLZ, K. DOOSTHOSEINI, A. TARMIAN (2016) Measurement of wood cutting forces during bandsawing using piezoelectric dynamometer. *Drvna Industrija* **67**(1) 79-84; DOI:10.5552/drind.2016.1433.
- [6] T. KRENKE, S. FRYBORT, U. MLLER (2017) Determining cutting force parameters by applying a system function. *Journal Machining Science and Technology* **21**(3) 436-451; DOI:org/10.1080/10910344.2017.1284563.
- [7] P. OBRESHKOV (1995) "Woodworking Machines". Publishing House "BM" (in Bulgarian).
- [8] B. MARINOV (2018) "Dynamic and Shock Processes in Some Classes of Woodworking Machines. Analysis and Optimization". Omniscryptum Publishing Group-Germany/LAP LAMBERT Academic Publishing.
- [9] B. MARINOV (2014) Spatial deformations in the transmissions of certain classes of woodworking machines. *Mechanism and Machine Theory* **82** 1-16; DOI: <http://dx9doi.org/10.1016/j.mechmachtheory.2014.07.010>.
- [10] A. PISAREV, Ts. PARASKOV, C. BACHVAROV (1988) "Course in Theoretical Mechanics. Second part-Dynamics". State Publishing House Technics (in Bulgarian).
- [11] R.M. DREIZLER, C.S. LÜDDE (2010) "Theoretical Mechanics: Theoretical Physics 1". Springer, Berlin, Heidelberg; DOI:10.1007/978-3-642-11138-9.
- [12] B. PORANKIEWICZ, B. AXELSSON, A. GRÖNLUND, B. MARKLUND (2011) Main and normal cutting forces by machining wood of pinus sylvestris. *Bio Resources* **6**(4) 3687-3713.
- [13] ZH. GOCHEV (2005) "Handbook for Exercise of Wood Cutting and Woodworking Tools", Publishing House in LTU (in Bulgarian).
- [14] R. PETERS (2006) "Band Saw Fundamentals: The Complete Guide", Hearst Communications Inc.
- [15] W. TURNER (2013) "A Comprehensive Handbook on Uses and Applications of the Band Saw and Jig Saw", Literary Licensing LLC.
- [16] Š. BARČÍK (2003) Experimental cutting on the table band-sawing machine. *European Journal of Wood and Wood Products* **61**(4) 313-320; DOI:10.1007/s00107-002-0342-9.
- [17] V. MILKOV (2008) "Strength of Materials (theory, tasks and software)". Technical University-Varna (in Bulgarian).
- [18] B. DUPEN (2014) "Applied Strength of Materials for Engineering Technology". Indiana University – Purdue University Fort Wayne.